

## Tomographic reconstruction of the density matrix via pattern functions

U. Leonhardt and H. Paul

*Arbeitsgruppe "Nichtklassische Strahlung" der Max-Planck-Gesellschaft  
an der Humboldt-Universität zu Berlin, Rudower Chaussee 5, 12484 Berlin, Germany*

G. M. D'Ariano

*Dipartimento di Fisica "A. Volta," via Bassi 6, I 27100 Pavia, Italy*

(Received 21 April 1995)

We propose a general method for reconstructing directly the density matrix of a single light mode in optical homodyne tomography. In our scheme the density matrix  $\langle a|\hat{\rho}|a'\rangle$  is obtained by averaging a set of pattern functions  $F_{aa'}(x_\theta, \theta)$  with respect to the homodyne data  $x_\theta$ . The functions show the typical features of the quadrature distributions for the corresponding density-matrix elements. It is also possible to compensate the effect of detection losses which requires, however, extra effort in both experimental and numerical precision. We calculate the pattern functions for the coherent-state and Fock representations and study their properties. We believe that our method is the most efficient way for reconstructing the density matrix from homodyne measurements.

PACS number(s): 42.50.Dv, 42.65.Ky, 03.65.Bz

### I. INTRODUCTION

One of the deep lessons we learned from quantum mechanics is that we cannot observe physical objects in their full complexity. In a single experiment we may see only particular aspects of a quantum object but not all of them simultaneously since some are complementary and hence mutually exclusive. The quantum state, however, comprises all facets of a physical object. Since von Neumann's classic book [1] and Fano's review [2], we are used to describing it by a density operator  $\hat{\rho}$ , while expectation values of observable quantities are traces  $\text{Tr}\{\hat{\rho}\hat{F}\}$  of  $\hat{\rho}$  and Hermitian operators  $\hat{F}$ . This formal difference reflects the general dualism of quantum mechanics—the distinction between physical states and observable quantities.

Although we cannot measure precisely the quantum state in a single experiment, we can perform different experiments on equally prepared objects and measure the various aspects separately. Then we may infer the quantum state from the recorded statistical distributions of the measured quantities. This general idea [3–6] was experimentally realized for the first time [7–10] in a quantum-optical scheme proposed by Vogel and Risken [11]. Quadrature distributions of equally prepared light pulses were measured by homodyne detection. The quadratures  $\hat{x}_\theta = \hat{x}\cos\theta + \hat{p}\sin\theta$  characterize the various quantum aspects of a single light mode modeled by a harmonic oscillator. Here  $\hat{x}$  and  $\hat{p}$  denote the appropriately normalized in-phase and out-of-phase components of the optical field. They represent the position and the momentum of a harmonic oscillator. The quadrature distributions  $w_\theta(x_\theta)$  are Radon transforms of the Wigner function  $W(x, p)$  [12],

$$w_\theta(x_\theta) = \int_{-\infty}^{+\infty} W(x_\theta \cos\theta - p_\theta \sin\theta, x_\theta \sin\theta + p_\theta \cos\theta) dp_\theta. \quad (1)$$

From the set of histograms  $w_\theta(x_\theta)$  the Wigner function can be tomographically reconstructed [7]. The Wigner function

[12] contains the complete information about the light mode. It can be used for calculating not precisely measurable quantities, such as the properties of the quantum-optical phase [13–15] or quantities that are otherwise difficult to observe. So it is a highly nontrivial experimental problem to measure precisely the photon-number distribution of nonclassical light fields. The Schleich-Wheeler oscillations [16] of a squeezed state, for instance, have not been observed yet.

The ultimate goal of the quantum-state detection is, however, the determination of the density matrix rather than the reconstruction of the Wigner function. Can we reconstruct the density matrix directly? Recently, D'Ariano, Macchiavello, and Paris [17] proposed a method for calculating the density matrix in Fock basis directly from the measured quadrature distributions. In numerical simulations [18] they tested the precision of their scheme for calculating photon-number and quantum-optical-phase properties. Munroe *et al.* [19] showed both theoretically and experimentally how to calculate the diagonal elements of the density matrix in Fock basis from phase-averaged quadrature histograms. These quantities contain all the information about the photon statistics of the field. Kühn, Welsch, and Vogel [20,21] derived formulas for reconstructing the density matrix in the position representation. In this paper we unify, generalize, and clarify these methods [22,23]. We demonstrate that the density matrix can be reconstructed in an arbitrary basis  $|a\rangle$ , using a set of pattern functions  $F_{aa'}(x_\theta; \theta)$ . The functions show the typical features of the density-matrix elements  $\langle a|\hat{\rho}|a'\rangle$  in quadrature distributions. These features and hence the matrix elements are detected by averaging the pattern functions with respect to the measured quadrature histograms. Moreover, losses in detection efficiency [24] can be compensated for up to certain limits [22,25,26]. For this, the pattern functions must be more pronounced. The compensation of losses, however, requires extra effort in both experimental and numerical precision, as one would expect.

We begin in Sec. II with a brief technical survey on the relation of quadrature histograms to the density operator.

Some of the material can be found in the enormous amount of literature on quasiprobability distributions, which is the common property of the quantum-optics community nowadays. We apologize for not quoting the discoveries of particular formal relations. Section III contains the central results of our paper. The pattern functions  $F_{aa'}(x_\theta; \theta)$  are introduced and analyzed for the coherent-state and Fock representation, respectively. Numerical simulations illustrate the reconstruction of the Schleich-Wheeler oscillations [16] for highly squeezed states.

## II. RELATING THE DENSITY OPERATOR TO QUADRATURE DISTRIBUTIONS

Let us consider some formal relations among the density operator, the characteristic function, and marginal distributions of  $s$ -parametrized quasiprobability distributions [27]. The last are the quadrature histograms measured in realistic experiments [24,10]. We are going to relate these distributions to the density operator in various ways that are convenient for later explicit calculations. We start with the definition of the characteristic function

$$\tilde{W}(\zeta_1, \zeta_2) \equiv \text{Tr}\{\hat{\rho} \exp(-i\zeta_1 \hat{x} - i\zeta_2 \hat{p})\} \quad (2)$$

and its relation to the density operator

$$\hat{\rho} = \frac{1}{2\pi} \int_{-\infty}^{+\infty} \int_{-\infty}^{+\infty} \exp(i\zeta_1 \hat{x} + i\zeta_2 \hat{p}) \tilde{W}(\zeta_1, \zeta_2) d\zeta_1 d\zeta_2. \quad (3)$$

This expression is sometimes called the Weyl formula since it is associated with Weyl's quantization method [28]. We define  $s$ -parametrized quasiprobability distributions  $W(x, p; s)$  as Fourier transforms of the corresponding characteristic functions

$$\tilde{W}(\zeta_1, \zeta_2; s) \equiv \tilde{W}(\zeta_1, \zeta_2) \exp\left[\frac{s}{4}(\zeta_1^2 + \zeta_2^2)\right], \quad (4)$$

so that

$$W(x, p; s) \equiv \frac{1}{(2\pi)^2} \int_{-\infty}^{+\infty} \int_{-\infty}^{+\infty} \exp(i\zeta_1 x + i\zeta_2 p) \times \tilde{W}(\zeta_1, \zeta_2; s) d\zeta_1 d\zeta_2. \quad (5)$$

Marginal distributions  $w_\theta(x_\theta; s)$  are obtained by the Radon transforms of the  $s$ -parametrized quasiprobability distributions in the same way as the marginals of the Wigner function [see Eq. (1)]. Comparing the Fourier-transformed marginal distribution

$$\tilde{w}_\theta(\zeta; s) \equiv \int_{-\infty}^{+\infty} \exp(-i\zeta x_\theta) w_\theta(x_\theta; s) dx_\theta \quad (6)$$

with the characteristic function  $\tilde{W}(\zeta_1, \zeta_2; s)$ , we reproduce the central formula for optical homodyne tomography [11,9],

$$\tilde{w}_\theta(\zeta; s) = \tilde{W}(\zeta \cos\theta, \zeta \sin\theta; s). \quad (7)$$

The set of Fourier-transformed marginal distributions is equal to the characteristic function in polar coordinates. Substituting this in the Weyl formula (3) gives us

$$\tilde{\rho} = \frac{1}{2\pi} \int_0^\pi \int_{-\infty}^{+\infty} \exp\left(i\zeta \hat{x}_\theta - \frac{s}{4}\zeta^2\right) \tilde{w}_\theta(\zeta; s) |\zeta| d\zeta d\theta \quad (8)$$

with the quadrature operator

$$\hat{x}_\theta = \hat{x} \cos\theta + \hat{p} \sin\theta = \hat{U}^\dagger(\theta) \hat{x} \hat{U}(\theta) \quad (9)$$

and the phase shifter

$$\hat{U}(\theta) = \exp(-i\theta \hat{a}^\dagger \hat{a}). \quad (10)$$

As usual,  $\hat{a} = 2^{-1/2}(\hat{x} + i\hat{p})$  denotes the annihilation operator. Utilizing the definition (6) of the  $\tilde{w}_\theta(\zeta; \theta)$  function, we obtain our first formula relating the density operator  $\hat{\rho}$  to marginals of  $s$ -parametrized quasiprobability distributions

$$\hat{\rho} = \int_0^\pi \int_{-\infty}^{+\infty} w_\theta(x_\theta; s) K(\hat{x}_\theta - x_\theta; s) dx_\theta d\theta \quad (11)$$

with the kernel

$$K(\hat{x}_\theta - x_\theta; s) = \hat{U}^\dagger(\theta) K(\hat{x} - x_\theta; s) \hat{U}(\theta) \quad (12)$$

and

$$K(\hat{x}; s) = \frac{1}{2\pi} \int_{-\infty}^{+\infty} \exp\left(i\zeta \hat{x} - \frac{s}{4}\zeta^2\right) |\zeta| d\zeta. \quad (13)$$

We express the kernel by using the Baker-Hausdorff formula

$$\begin{aligned} \exp(i\zeta \hat{x}) &= \exp\left[i\frac{\zeta}{\sqrt{2}}(\hat{a} + \hat{a}^\dagger)\right] \\ &= \exp\left(i\frac{\zeta}{\sqrt{2}}\hat{a}^\dagger\right) \exp\left(i\frac{\zeta}{\sqrt{2}}\hat{a}\right) \exp\left(-\frac{\zeta^2}{4}\right) \end{aligned} \quad (14)$$

and obtain

$$\begin{aligned} K(\hat{x} - x_\theta; s) &= \frac{1}{2\pi} \int_{-\infty}^{+\infty} \exp\left(-\frac{1+s}{4}\zeta^2 - i\zeta x_\theta\right) \exp\left(i\frac{\zeta}{\sqrt{2}}\hat{a}^\dagger\right) \exp\left(i\frac{\zeta}{\sqrt{2}}\hat{a}\right) |\zeta| d\zeta \\ &= \frac{1}{2\pi} \int_{-\infty}^{+\infty} \exp\left(-\frac{1+s}{4}\zeta^2 - i\zeta x_\theta\right) \exp(i\zeta \hat{x}) : |\zeta| d\zeta. \end{aligned} \quad (15)$$

As usual  $::$  is the normal-ordering symbol. This expression will be helpful in deriving explicit formulas for the density operator in the Fock basis. We solve the integral in Eq. (15),

$$\begin{aligned} h_1(x) &= \frac{1}{2\pi} \left( \int_0^{+\infty} - \int_{-\infty}^0 \right) \exp\left(-\frac{\xi^2}{4} + ix\xi\right) \xi d\xi \\ &= \frac{2}{\pi} [1 - \pi^{1/2} x \exp(-x^2) \operatorname{erfi}(x)], \end{aligned} \quad (16)$$

with the imaginary error function  $\operatorname{erfi}(x) = 2\pi^{-1/2} \int_0^x \exp(t^2) dt$ , and obtain a compact expression for the kernel

$$K(\hat{x}_\theta - x_\theta; s) = \frac{1}{1+s} : h_1((1+s)^{-1/2}(\hat{x}_\theta - x_\theta)) :. \quad (17)$$

In the special case  $s=0$  (when we consider marginals of the Wigner function) we obtain from Eq. (13) another simple expression for the kernel,

$$K(\hat{x}) \equiv K(\hat{x}; 0) = \frac{1}{\pi} \int_0^\infty \cos(\xi \hat{x}) \xi d\xi = -\frac{1}{\pi} \frac{P}{\hat{x}^2}. \quad (18)$$

In this case the kernel is a generalized function of the position operator  $\hat{x}$  [29]. It is well defined only with respect to integrations in which the kernel occurs, and the symbol  $P$  means that Cauchy's principle value should be taken from such integrals. Finally we note that the  $s$ -parametrized kernels are related to each other by

$$K(\hat{x}; s_2) = \exp\left(\frac{s_2 - s_1}{4} \frac{\partial^2}{\partial \hat{x}^2}\right) K(\hat{x}; s_1), \quad (19)$$

as is easily obtained from Eq. (13). Now we are prepared to derive explicit formulas for reconstructing the density matrix in a given basis.

### III. RECONSTRUCTING THE DENSITY MATRIX

The abstract density operator  $\hat{\rho}$  is a useful construction for performing basis-independent calculations in quantum theory. Here we are interested in the reconstruction of the quantum state from measurements, which requires the specification of the density matrix in a given basis  $\{|a\rangle\}$ . We obtain from our general reconstruction formula (11)

$$\langle a | \hat{\rho} | a' \rangle = \int_0^\pi \int_{-\infty}^{+\infty} w_\theta(x_\theta; s) F_{aa'}(x_\theta, \theta; s) dx_\theta d\theta \quad (20)$$

with

$$F_{aa'}(x_\theta, \theta; s) = \langle a | K(\hat{x}_\theta - x_\theta) | a' \rangle. \quad (21)$$

This means that a set of  $F_{aa'}(x_\theta, \theta; s)$  functions should be averaged with respect to the recorded distributions to yield the density matrix  $\langle a | \hat{\rho} | a' \rangle$ . The statistical distributions  $w_\theta(x_\theta; s)$  measured in realistic homodyne experiments [24] are characterized in terms of the overall detection efficiency  $\eta$  by the simple formula

$$s = 1 - \eta^{-1}. \quad (22)$$

Before we derive explicit expressions for the  $F_{aa'}(x_\theta, \theta; s)$  functions in the coherent-state and Fock representations, respectively, we note that the  $F_{aa'}$  depend in a simple way on the quadrature wave functions when  $s=0$ , i.e., when the detection efficiency is unity. In fact, we obtain from Eqs. (12) and (18)

$$F_{aa'}(x_\theta, \theta) \equiv F_{aa'}(x_\theta, \theta; 0) = -\frac{P}{\pi} \int_{-\infty}^{+\infty} \frac{\langle a | x; \theta \rangle \langle x; \theta | a' \rangle}{(x - x_\theta)^2} dx, \quad (23)$$

with  $|x; \theta\rangle$  being the quadrature eigenstates

$$|x; \theta\rangle = \hat{U}^\dagger(\theta) |x\rangle. \quad (24)$$

As already noted in Sec. II,  $P$  means that Cauchy's principle value is to be taken from the integral in Eq. (23). Since the kernel  $-P(x - x_\theta)^{-2}$  is concentrated around  $x = x_\theta$ , the  $F_{aa'}(x_\theta, \theta)$  functions should be similar to the product of the quadrature wave functions  $\langle a | x; \theta \rangle$  and  $\langle x; \theta | a' \rangle$ . They show the typical features of the quadrature distributions of the projectors  $|a'\rangle\langle a|$ . In view of this we call the  $F_{aa'}$  functions the *pattern functions* for the density-matrix elements  $\langle a | \hat{\rho} | a' \rangle$ . When the detection efficiency is less than unity, the pattern functions must compensate for the smoothing of the quadrature distributions by enhancing the patterns for the elements  $\langle a | \hat{\rho} | a' \rangle$ . In fact, we obtain from Eq. (19)

$$F_{aa'}(x_\theta, \theta) = \exp\left(-\frac{s}{4} \frac{\partial^2}{\partial x_\theta^2}\right) F_{aa'}(x_\theta, \theta; s), \quad (25)$$

which means that the pattern functions for perfect detection are smoothed pattern functions for the imperfect case where  $s$  is negative. Consequently, the  $F_{aa'}(x_\theta, \theta; s)$  show sharper features than the  $F_{aa'}(x_\theta, \theta)$  functions. We note however that the compensation of detection losses is possible only up to certain limits, which depend on the particular representation (see Ref. [22]). Then the pattern functions become singular. It has been conjectured [22] that the limit efficiency is always greater than or equal to  $\frac{1}{2}$ .

#### A. Coherent-state representation

Coherent states  $\{|\alpha\rangle\}$  form a convenient yet not orthonormal basis for the density operator of a harmonic oscillator. An infinite set of coherent states  $\{|\alpha\rangle\}$  with an accumulation point in the complex plane [30] or a lattice of coherent states [31] is sufficient to represent the quantum state. The coherent-state representation may be useful for detecting macroscopic quantum-interference phenomena in phase space [32]. To calculate the required pattern functions, we utilize some basic properties of coherent states,

$$\hat{a}|\alpha\rangle = \alpha|\alpha\rangle \quad (26)$$

and

$$\langle \alpha | \alpha' \rangle = \exp(-\frac{1}{2} |\alpha - \alpha'|^2) \quad (27)$$

and obtain immediately from Eq. (17)

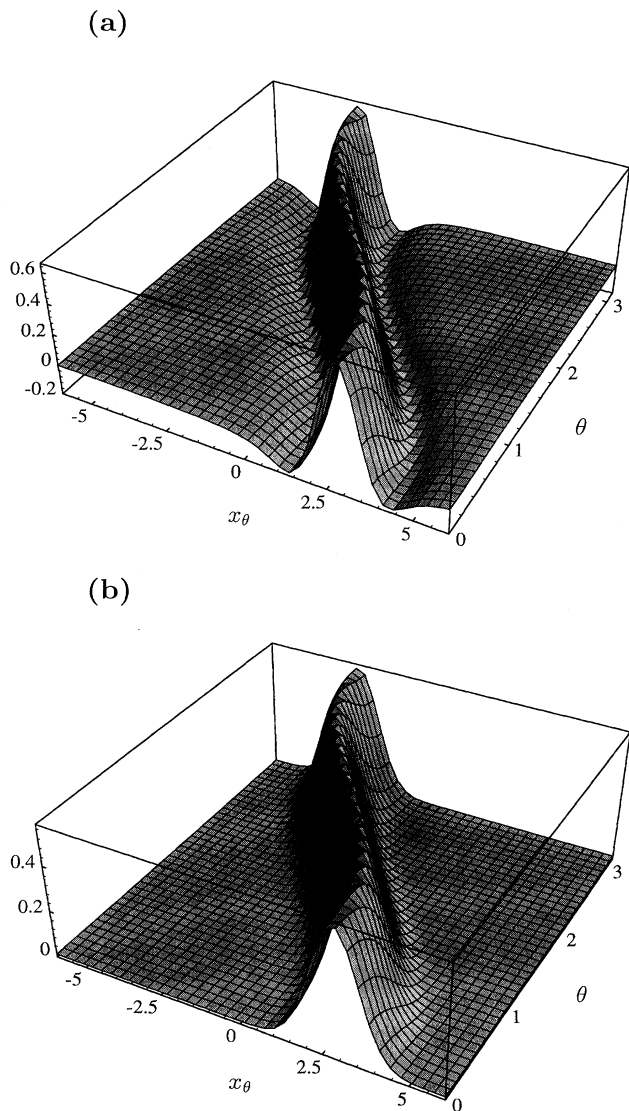


FIG. 1. Diagonal pattern function  $F_{\alpha\alpha}(x_\theta, \theta)$  (a) versus quadrature distribution  $|\psi_\alpha(x_\theta, \theta)|^2$  (b) of the coherent state  $|\alpha\rangle$  with  $\alpha=4$ . As is well known, the quadrature wave functions are  $\psi_\alpha(x_\theta, \theta) = \pi^{-1/4} \exp[-(x_\theta - \tilde{x}_\theta)^2/2 + i\tilde{p}_\theta x_\theta - i\tilde{x}_\theta \tilde{p}_\theta/2]$ , with  $\tilde{x}_\theta = 2^{-1/2}(\alpha^* e^{i\theta} + \alpha e^{-i\theta})$  and  $\tilde{p}_\theta = i2^{-1/2}(\alpha^* e^{i\theta} - \alpha e^{-i\theta})$ . The pattern function shows the typical features of the quadrature distribution.

$$F_{\alpha\alpha'}(x_\theta, \theta; s) = \frac{1}{1+s} h_1((1+s)^{-1/2}(\tilde{x}_\theta - x_\theta)) \times \exp(-\frac{1}{2}|\alpha - \alpha'|^2) \quad (28)$$

with

$$\tilde{x}_\theta = 2^{-1/2}(\alpha^* e^{i\theta} + \alpha' e^{-i\theta}). \quad (29)$$

The  $h_1$  function is defined in Eq. (16).

Figure 1 illustrates that the diagonal pattern functions  $F_{\alpha\alpha}(x_\theta, \theta)$  are, in fact, very similar to the quadrature distributions of the coherent states  $|\alpha\rangle$ . They follow the track of

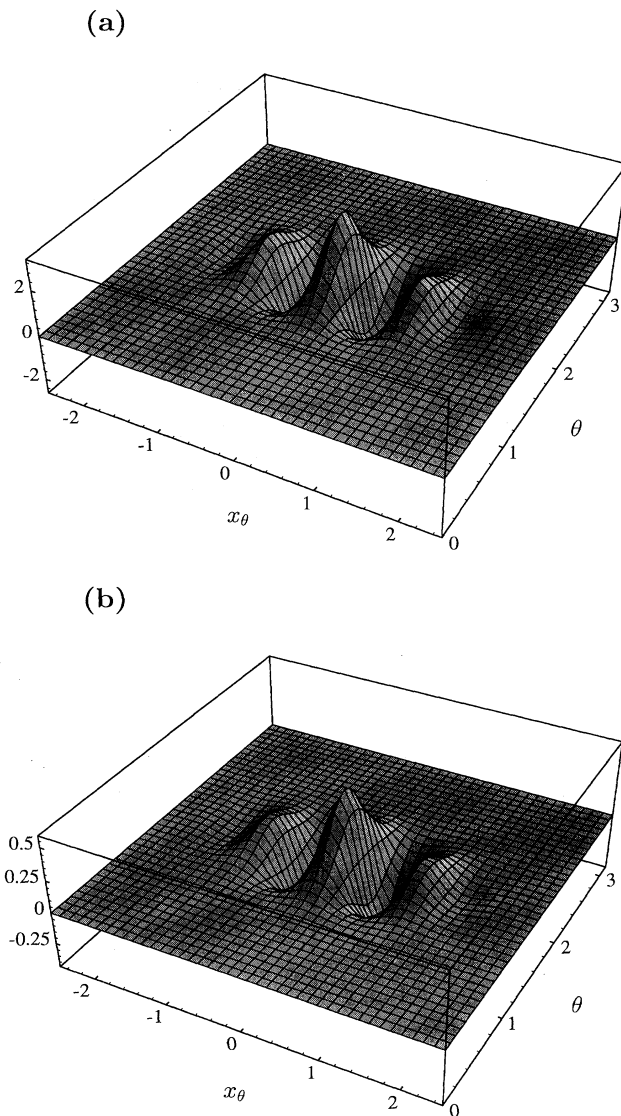


FIG. 2. Real part of the off-diagonal pattern function  $F_{\alpha, -\alpha}(x_\theta, \theta)$  (a) versus the real part of the wave-function product  $\psi_\alpha^*(x_\theta, \theta)\psi_{-\alpha}(x_\theta, \theta)$  (b) for  $\alpha=4$ . The figures are almost indistinguishable.

the harmonic evolution. So by averaging these functions with respect to the measured quadrature distribution, the coherent-state components with the right amplitudes and phases are picked out. Figure 2 shows clearly that the off-diagonal pattern functions exhibit typical oscillations. They correspond to the well-known Schrödinger-cat oscillations. This confirms that such oscillations are the most important features to detect when we are looking for quantum-coherence effects represented in the off-diagonal elements of the density matrix  $\langle a|\hat{\rho}|a'\rangle$ . When the detection efficiency is less than unity, the parameter  $s$  is less than zero. As is easily seen from Eq. (28), the pattern functions are pronounced until  $s$  reaches  $-1$ , i.e., until  $\eta$  reaches the critical value  $\frac{1}{2}$ . Then the  $h_1$  function is no longer bounded and cannot be used in general for averaging with respect to quadrature distributions.

### B. Fock representation

The favorite basis in the quantum-optics community is still the Fock basis  $\{|n\rangle\}$ . We are going to calculate explicit expressions for the Fock pattern functions, which appear as significantly simplified versions of the earlier results by D'Ariano, Macchiavello, and Paris [17]. First, we see from Eq. (12) that the phase dependence of the pattern functions is trivial,

$$F_{nn'}(x_\theta, \theta; s) = \exp[i(n-n')\theta] f_{nn'}(x_\theta; s). \quad (30)$$

We obtain from Eq. (15) that the  $f_{nn'}(x_\theta; s)$  are given by the expression

$$f_{nn'}(x_\theta; s) = \frac{1}{2\pi} \int_{-\infty}^{+\infty} \exp\left(-\frac{1+s}{4}\zeta^2 - i\zeta x_\theta\right) \left\langle n \left| \exp\left(i\frac{\zeta}{\sqrt{2}}\hat{a}^\dagger\right) \exp\left(i\frac{\zeta}{\sqrt{2}}\hat{a}\right) \right| n' \right\rangle |\zeta| d\zeta. \quad (31)$$

We use the property

$$\hat{a}^\nu |n\rangle = \left[\frac{n!}{(n-\nu)!}\right]^{1/2} |n-\nu\rangle \quad (32)$$

of the Fock states and get

$$\left\langle n \left| \exp\left(i\frac{\zeta}{\sqrt{2}}\hat{a}^\dagger\right) \exp\left(i\frac{\zeta}{\sqrt{2}}\hat{a}\right) \right| n' \right\rangle = \sum_{\nu=0}^n \sum_{\nu'=0}^{n'} \left(i\frac{\zeta}{\sqrt{2}}\right)^{\nu+\nu'} \frac{1}{\nu!\nu'} \left[\frac{n!n'!}{(n-\nu)!(n'-\nu)!}\right]^{1/2} \langle n-\nu | n'-\nu' \rangle. \quad (33)$$

Since the Fock states are orthonormal, we have  $\nu' = \nu + n' - n$  and obtain for  $n' \geq n$

$$f_{nn'}(x_\theta; s) = (n!n'!)^{1/2} 2^{(n-n')/2} \sum_{\nu=0}^n \frac{h_{2\nu+n'-n+1}(x_\theta; s)}{2^\nu \nu! (n-\nu)! (n'-n+\nu)!}. \quad (34)$$

The  $h_n$  functions are defined by

$$\begin{aligned} h_n(x; s) &\equiv \frac{1}{2\pi i} \left( \int_0^{+\infty} - \int_{-\infty}^0 \right) (i\zeta)^n \exp\left(-\frac{1+s}{4}\zeta^2 - i\zeta x\right) d\zeta \\ &= \frac{1}{\pi} \operatorname{Im} \left[ \int_0^{\infty} (i\zeta)^n \exp\left(-\frac{1+s}{4}\zeta^2 - i\zeta x\right) d\zeta \right]. \end{aligned} \quad (35)$$

Since the  $h_n$  functions are real, the  $f_{nn'}$  are real as well and we can simply use the relation

$$f_{nn'}(x_\theta; s) = f_{n'n}(x_\theta; s) \quad (36)$$

for  $n' < n$ .

We are going to show some properties of the  $h_n$  functions. First, they exist if  $s > -1$  (if the detection efficiency exceeds  $\frac{1}{2}$ ). We obtain from the integral representation (35) the scaling property

$$h_n(x; s) = (1+s)^{-(n+1)/2} h_n((1+s)^{-1/2} x) \quad (37)$$

with

$$h_n(x) \equiv h_n(x; 0). \quad (38)$$

We can express the  $h_n$  in terms of parabolic cylinder functions, using Ref. [33] (Vol. I, Eq. 2.3.15.3),

$$h_n(x) = \frac{n!}{\pi} 2^{(n+1)/2} \exp\left(-\frac{x^2}{2}\right) \operatorname{Im}[i^n D_{-n-1}(-ix\sqrt{2})]. \quad (39)$$

We derive

$$h_{n+1}(x) - 2xh_n(x) + 2nh_{n-1}(x) = 0 \quad (40)$$

from the recurrence relation of the parabolic cylinder functions [34], Eq. 8.2.(14). This means that the  $h_n$  functions obey the recurrence relation of the Hermite polynomials. They are, however, expressions in terms of the imaginary error function  $\operatorname{erfi}(x) = 2\pi^{-1/2} \int_0^x \exp(t^2) dt$  and of polynomials since the initial functions are given by

$$h_0(x) = -\pi^{-1/2} \exp(-x^2) \operatorname{erfi}(x) \quad (41)$$

and by Eq. (16) for  $h_1(x)$ . Note that the recurrence relation (40) may be used for calculating the  $f_{nn'}$  functions numerically. From the asymptotic expansion of the parabolic cylinder functions, Eq. 8.4.(1) of Ref. [34], we obtain the asymptotic behavior of the  $h_n$  functions

$$h_n(x) \sim -\frac{1}{\pi x^{n+1}}. \quad (42)$$

The  $h_n$  functions decay algebraically. Hence the leading term in the expression (34) for the  $f_{nn'}$  function is

$$f_{nn'}(x_\theta; s) \sim (1+s)^{(n'-n+1)/2} f_{nn'}(x_\theta), \quad (43)$$

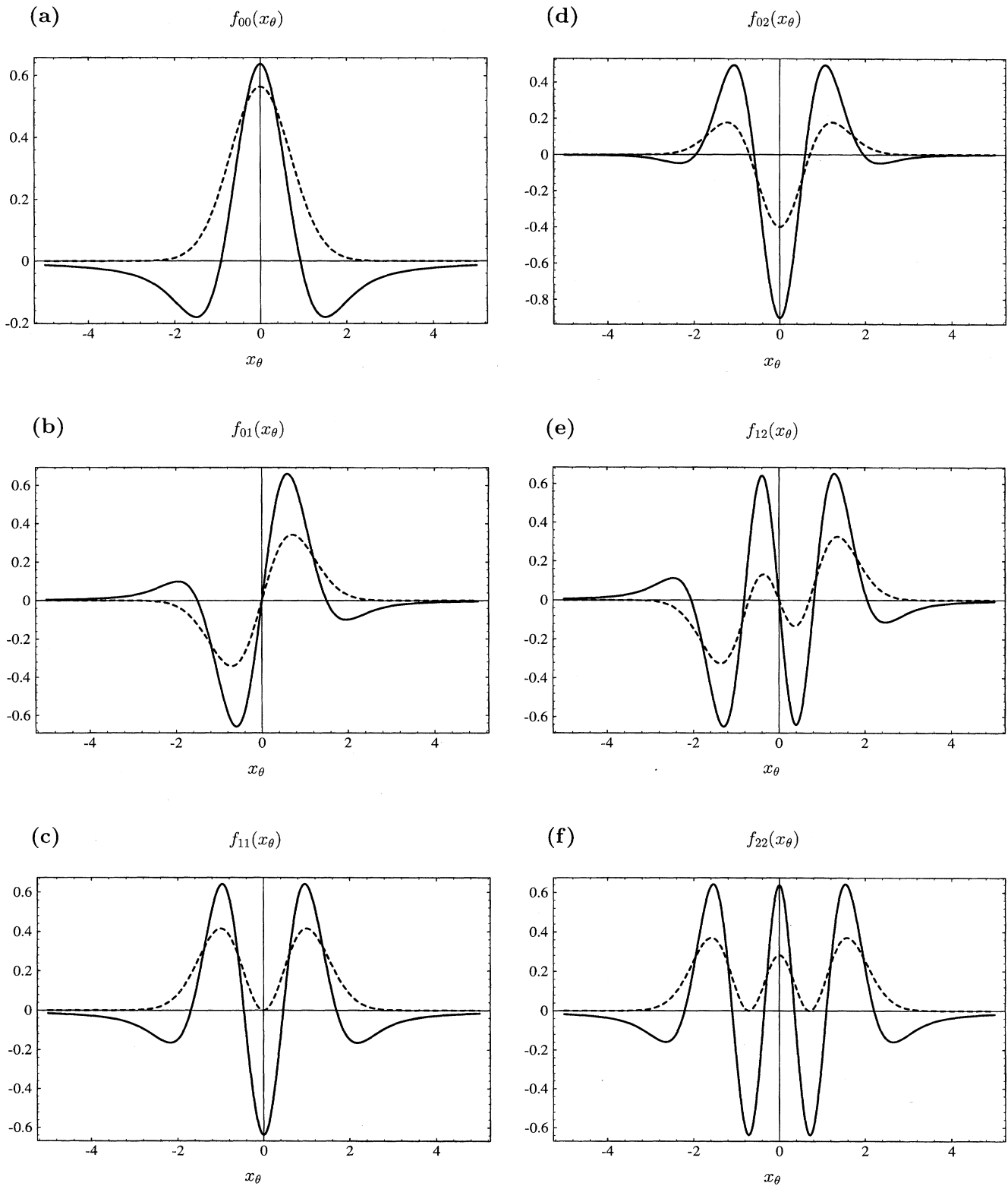


FIG. 3. Some  $f_{nn'}(x_\theta)$  functions (lines) versus the products of the wave functions  $\psi_n^*(x_\theta)$  and  $\psi_{n'}(x_\theta)$  (dashed lines) of the Fock states for (a)  $n=0, n'=0$ ; (b)  $n=0, n'=1$ ; (c)  $n=1, n'=1$ ; (d)  $n=0, n'=2$ ; (e)  $n=1, n'=2$ ; and (f)  $n=2, n'=2$ . The Schrödinger wave functions are given by  $\psi_n(x_\theta) = (2^n n! \sqrt{\pi})^{-1/2} \exp(-x_\theta^2/2) H_n(x_\theta)$  with the Hermite polynomials  $H_n$ . As in Figs. 1 and 2, the pattern functions pronounce the typical features of the corresponding quadrature wave functions.

$$f_{nn'}(x) \sim - \left( \frac{n'!}{n!} \right)^{1/2} (n' - n + 1) 2^{-n/2} \frac{1}{\pi x^{n' - n + 2}}. \quad (44)$$

The pattern functions decay like  $x^{-(n' - n + 2)}$  with  $n' \geq n$ . Thus the integral in the basic relation (20) exists for physical states having normalizable quadrature distributions.

Some of the  $f_{nn'}$  functions are depicted in Fig. 3 and compared with the product of the Schrödinger wave functions  $\psi_n^*(x)$  and  $\psi_{n'}(x)$  of the corresponding Fock states  $|n\rangle$  and  $|n'\rangle$ . It is evident that they show just the typical features of  $\psi_n^*(x)\psi_{n'}(x)$ . In this way they guarantee that the right matrix elements are picked out when the pattern functions are averaged with respect to the measured quadrature distributions.

### C. Simulations

The Schleich-Wheeler oscillations in the photon distributions of squeezed states are manifestations of interference in phase space [16]. They are extremely difficult to measure directly, but they can be inferred from quadrature distributions by using our method. We performed numerical simulations to test our scheme as well as to estimate the experimental effort needed. The photon-number distribution for a squeezed state with the Wigner function

$$W(x, p) = \pi^{-1} \exp[-s(x - \alpha\sqrt{2})^2 - s^{-1}p^2] \quad (45)$$

is given by [16]

$$\langle n | \hat{\rho} | n \rangle = \left( \frac{c^2 - 1}{c^2} \right)^{1/2} \frac{c^{-n}}{2^n n!} H_n^2 \left( \frac{c+1}{\sqrt{2c}} \alpha \right) \exp \left( - \frac{c+1}{c} \alpha^2 \right) \quad (46)$$

with

$$c = \frac{s+1}{s-1}. \quad (47)$$

Figure 4(a) shows this distribution for the parameters  $s=20$  and  $\alpha=3$ .

We did computer experiments simulating 100 quadrature measurements for each phase  $\theta$ . The photon-number distribution was obtained by averaging the pattern functions  $F_{nn}(x_\theta, \theta)$  with respect to the “experimental data.” We did this ten times to estimate the error bars, and produced the photon distribution depicted in Fig. 4(b). It turns out that quite a few quadrature phases are required to reproduce the theoretical distribution (46). Figure 4(b), for instance, was obtained by using 260 phases. Perfect agreement with theory [Fig. 4(a)] was achieved with 2600 phases. So experimentalists should perform homodyne measurements with a large number of quadrature phases for reconstructing the Schleich-Wheeler oscillations or, alternatively, use a local oscillator with random phase [19].

We had some problems with the numerical precision in calculating the pattern functions  $F_{nn}(x_\theta, \theta)$  for large quantum numbers  $n, m > 20$ . In this case our expressions involve the cancellation of large numbers, which is a major source of numerical inaccuracy. We solved this problem by calculating the functions with extremely high precision before doing the

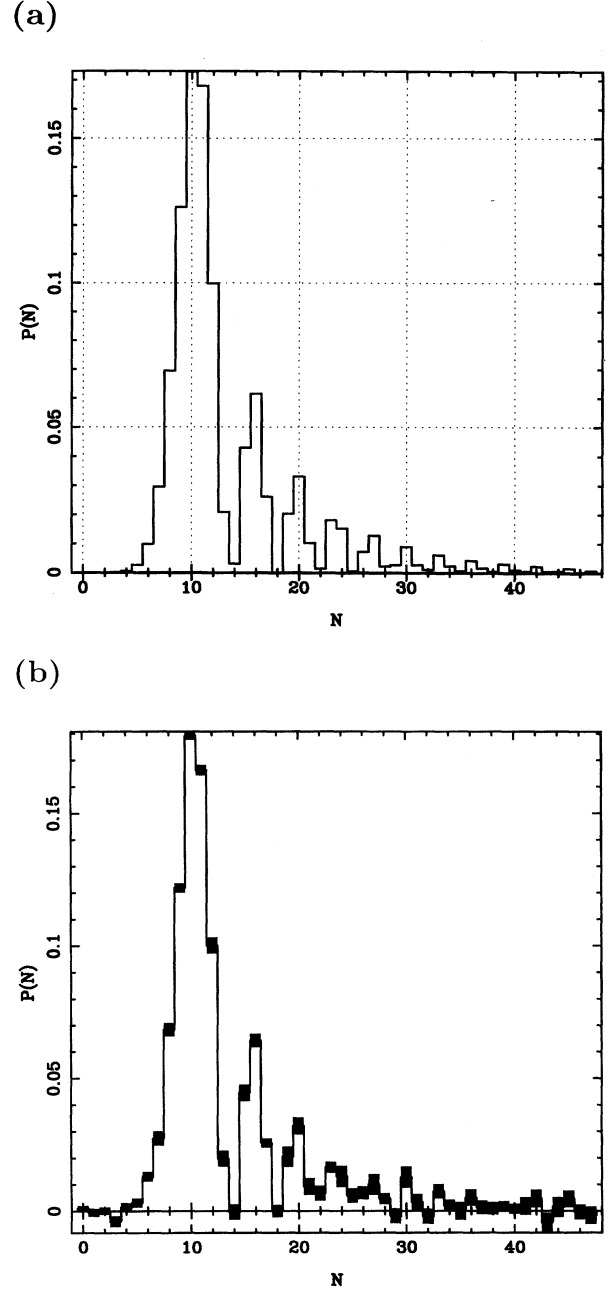


FIG. 4. (a) Photon-number distribution of the squeezed state (45) with the parameters  $s=20$  and  $\alpha=3$ . It shows the Schleich-Wheeler oscillations. (b) Reconstruction of this distribution from computer experiments using 260 quadrature phases with 100 measurements for each phase. The error bars have been obtained by comparing ten simulations.

simulations, and then did interpolations between the stored values. We believe, however, that this difficulty can be finally circumvented by using asymptotic methods in the case of large quantum numbers.

### IV. SUMMARY

We propose a general method for reconstructing directly the density matrix of a single light mode in optical homo-

dyme tomography. For this a set of pattern functions should be averaged with respect to the homodyne data. The pattern functions show the typical features of the quadrature distributions for the density-matrix elements. We calculated explicit expressions for the coherent state and the Fock representation. In our scheme it is also possible to compensate for the effect of detection losses, provided the detection efficiency exceeds certain limits [22]. The pattern functions should be changed in such a way that they show more pronounced features to compensate for the smoothing of the quadrature distributions. This requires, however, extra effort in both experimental and numerical precision. Some simulations illustrate the feasibility of our method, as well as the numerical limitations. We believe that our method is the most efficient way for reconstructing the density matrix from homodyne measurements. In particular, we would like to stress that our scheme compares favorably with conventional optical homodyne tomography [7] since in determining the

density operator it avoids the detour via the Wigner function, which requires at least one or, in general, two additional integral transformations. Moreover, our procedure is superior from the mathematical point of view, as there is no need for back-projection filtering that limits the resolution for the reconstruction of the Wigner function, as has been emphasized already in Ref. [17].

*Note added in proof.* Recently, a much more elegant and numerically stable formula for the Fock pattern functions has been discovered by Th. Richter (unpublished) and U. Leonhardt, M. Munroe, T. Kiss, M. G. Raymer, and Th. Richter (unpublished).

#### ACKNOWLEDGMENTS

We thank U. Herzog, U. Janicke, I. Jex, T. Kiss, M. Munroe, M. G. Raymer, Th. Richter, S. Stenholm, J. A. Vaccaro, and M. Wilkens for their helpful comments.

- 
- [1] J. von Neumann, *Mathematical Foundations of Quantum Mechanics* (Princeton University Press, Princeton, 1955).
- [2] U. Fano, *Rev. Mod. Phys.* **29**, 74 (1957).
- [3] The problem of whether the wave function can be reconstructed from position and momentum distributions was raised by W. Pauli in his article in the *Encyclopedia of Physics* (Springer, Berlin, 1958), Vol. 5, p. 17. See W. Gale, E. Guth, and G. T. Trammell, *Phys. Rev.* **165**, 1434 (1968); J. V. Corbett and C. A. Hurst, *J. Aust. Math. Soc. B* **20**, 182 (1978); A. Orłowski and H. Paul, *Phys. Rev. A* **50**, R921 (1994). Z. Białynicka-Birula and I. Białynicki-Birula, *J. Mod. Opt.* **41**, 2203 (1994), studied the Pauli problem for photon number and phase.
- [4] To our knowledge mostly theoretical work was done on the quantum-state reconstruction problem. Fano [2] suggested a general scheme for reconstructing the density matrix from a set of measured quantities that correspond to orthogonal operators. W. Band and J. L. Park, *Found. Phys.* **1**, 133 (1970); **1**, 211 (1971); **1**, 339 (1971); *Am. J. Phys.* **47**, 188 (1979), developed a method to find a set of observables for the state reconstruction and gave explicit examples for spin- $\frac{1}{2}$ , spin-1, and one-dimensional spinless systems. I. D. Ivanović, *J. Math. Phys.* **24**, 1199 (1983), refined this scheme. Based on another paper by I. D. Ivanović, *J. Phys. A* **14**, 3241 (1981), Wootters considered the quantum-state reconstruction for finite-dimensional systems; see W. K. Wootters, *Found. Phys.* **16**, 391 (1986); *Ann. Phys. (N.Y.)* **176**, 1 (1987); W. K. Wootters and B. D. Fields, *ibid.* **191**, 363 (1989). U. Larsen, *J. Phys. A* **23**, 1041 (1990), related it to the concept of complementary aspects. A. Royer, *Phys. Rev. Lett.* **55**, 2745 (1985); *Found. Phys.* **19**, 3 (1989); J. Bertrand and P. Bertrand, *ibid.* **17**, 397 (1987), considered schemes for measuring the Wigner function.
- [5] Recent experimental proposals for measuring the quantum state of radiation can be found in M. Wilkens and P. Meystre, *Phys. Rev. A* **43**, 3832 (1991); S. M. Dutra and P. L. Knight, *ibid.* **49**, 1506 (1994); M. Freyberger and A. M. Herkommer, *Phys. Rev. Lett.* **72**, 1952 (1994); B. Baseia, G. C. Marques, and V. S. Bagnato, *Phys. Lett. A* **200**, 7 (1995); P. J. Bardroff, E. Mayr, and W. P. Schleich, *Phys. Rev. A* **51**, 4963 (1995).
- [6] Quantum-state tomography for finite-dimensional systems was proposed by U. Leonhardt, *Phys. Rev. Lett.* **74**, 4101 (1995).
- [7] D. T. Smithey, M. Beck, M. G. Raymer, and A. Faridani, *Phys. Rev. Lett.* **70**, 1244 (1993); D. T. Smithey, M. Beck, J. Cooper, M. G. Raymer, and A. Faridani, *Phys. Scr.* **T48**, 35 (1993).
- [8] M. G. Raymer, D. T. Smithey, M. Beck, M. E. Anderson, and D. F. McAlister, in *Proceedings of the Third International Wigner Symposium, 1993*, *Int. J. Mod. Phys. B* (to be published).
- [9] Schemes for measuring the quantum state of light are reviewed in U. Leonhardt and H. Paul, *Prog. Quantum Electron.* **19**, 89 (1995).
- [10] Recently, the experimental reconstruction of the Wigner function for molecular oscillations was reported by T. J. Dunn, I. A. Walmsley, and S. Mukamel, *Phys. Rev. Lett.* **74**, 884 (1995).
- [11] K. Vogel and H. Risken, *Phys. Rev. A* **40**, 2847 (1989).
- [12] E. P. Wigner, *Phys. Rev.* **40**, 749 (1932). The Wigner representation is reviewed in V. I. Tatarskii, *Usp. Fiz. Nauk.* **139**, 587 (1983) [*Sov. Phys. Usp.* **26**, 311 (1983)]; and in M. Hillery, R. F. O'Connell, M. O. Scully, and E. P. Wigner, *Phys. Rep.* **106**, 121 (1984).
- [13] The phase problem in quantum optics is nicely reviewed in S. M. Barnett and B. J. Dalton, *Phys. Scr.* **T48**, 13 (1993); and R. Lynch, *Phys. Rep.* **256**, 367 (1995).
- [14] M. Beck, D. T. Smithey, and M. G. Raymer, *Phys. Rev. A* **48**, R890 (1993); M. Beck, D. T. Smithey, J. Cooper, and M. G. Raymer, *Opt. Lett.* **18**, 1259 (1993); D. T. Smithey, M. Beck, J. Cooper, and M. G. Raymer, *Phys. Rev. A* **48**, 3159 (1993).
- [15] In the phase-measurement schemes reviewed in Ref. 9 noisy canonical phases are measured; see U. Leonhardt, J. A. Vaccaro, B. Böhmer, and H. Paul, *Phys. Rev. A* **51**, 84 (1995).
- [16] W. Schleich and J. A. Wheeler, *Nature (London)* **326**, 574 (1987); *J. Opt. Soc. Am. B* **4**, 1715 (1987).
- [17] G. M. D'Ariano, C. Macchiavello, and M. G. A. Paris, *Phys. Rev. A* **50**, 4298 (1994).
- [18] G. M. D'Ariano, C. Macchiavello, and M. G. A. Paris, *Phys. Lett. A* **195**, 31 (1994).



- [19] M. Munroe, D. Boggavarapu, M. E. Anderson, and M. G. Raymer, *Phys. Rev. A* **52**, R924 (1995).
- [20] H. Kühn, D.-G. Welsch, and W. Vogel, *J. Mod. Opt.* **41**, 1607 (1994).
- [21] H. Kühn, D.-G. Welsh, and W. Vogel, *Phys. Rev. A* **51**, 4240 (1995), studied theoretically the state reconstruction of multi-mode light fields; see also Ref. [8].
- [22] For a first communication on our scheme see G. M. D'Ariano, U. Leonhardt, and H. Paul, *Phys. Rev. A* **52**, R1801 (1995). Here also the critical detection efficiencies have been considered.
- [23] For an alternative derivation of our results see H. Paul, U. Leonhardt, and G. M. D'Ariano, *Acta Phys. Slovaca* **45**, 261 (1995).
- [24] U. Leonhardt and H. Paul, *Phys. Rev. A* **48**, 4598 (1993).
- [25] An alternative loss-compensation method has been developed in T. Kiss, U. Leonhardt, and U. Herzog, *Acta Phys. Slovaca* **45**, 379 (1995); T. Kiss, U. Herzog, and U. Leonhardt, *Phys. Rev. A* **52**, 2433 (1995).
- [26] The overall quantum efficiency of a homodyne detector can be enhanced by using squeezed preamplification, which, however, is difficult to realize experimentally; see U. Leonhardt and H. Paul, *Phys. Rev. Lett.* **72**, 4086 (1994).
- [27] K. E. Cahill and R. J. Glauber, *Phys. Rev.* **177**, 1882 (1969).
- [28] H. Weyl, *Z. Phys.* **46**, 1 (1927); see also H. Weyl, *The Theory of Groups and Quantum Mechanics* (Dover, New York, 1950).
- [29] I. M. Gel'fand and G. E. Shilov, *Generalized Functions* (Academic, San Diego, 1965).
- [30] K. E. Cahill, *Phys. Rev. B* **138**, 1566 (1965).
- [31] H. Bacry, A. Grossmann, and J. Zak, *Phys. Rev. B* **12**, 1118 (1975).
- [32] V. Bužek and P. L. Knight, *Prog. Opt.* (to be published).
- [33] A. P. Prudnikov, Yu. A. Brychkov, and O. I. Marichev, *Integrals and Series* (Gordon and Breach, New York, 1992).
- [34] A. Erdélyi, *Higher Transcendental Functions* (McGraw-Hill, New York, 1955).

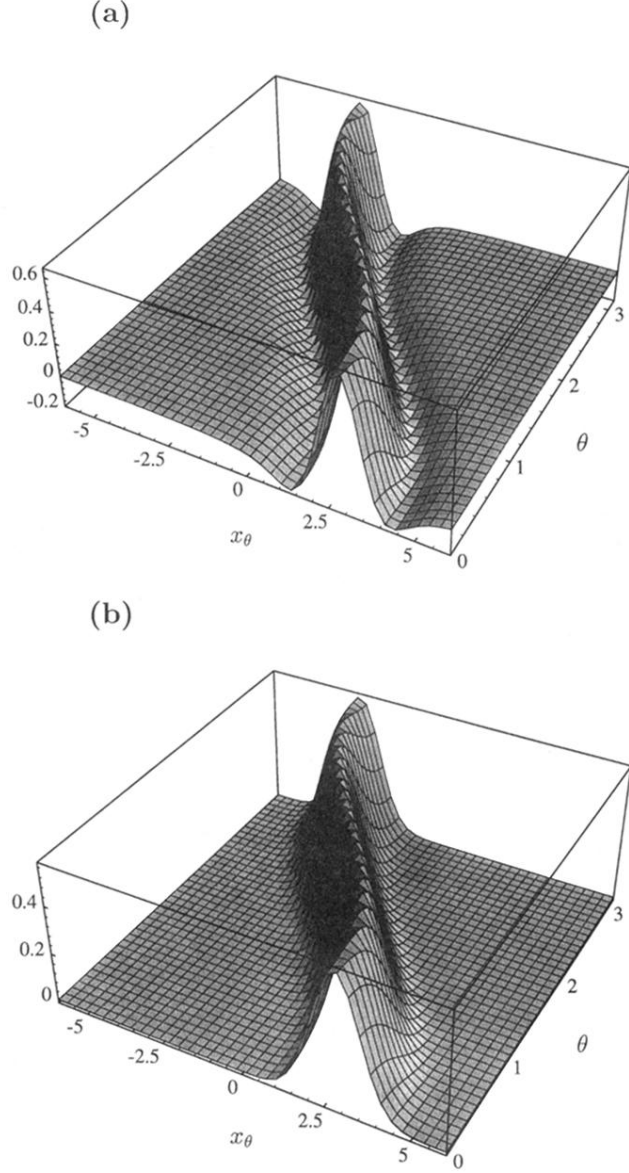


FIG. 1. Diagonal pattern function  $F_{\alpha\alpha}(x_\theta, \theta)$  (a) versus quadrature distribution  $|\psi_\alpha(x_\theta, \theta)|^2$  (b) of the coherent state  $|\alpha\rangle$  with  $\alpha=4$ . As is well known, the quadrature wave functions are  $\psi_\alpha(x_\theta, \theta) = \pi^{-1/4} \exp[-(x_\theta - \tilde{x}_\theta)^2/2 + i\tilde{p}_\theta x_\theta - i\tilde{x}_\theta \tilde{p}_\theta/2]$ , with  $\tilde{x}_\theta = 2^{-1/2}(\alpha^* e^{i\theta} + \alpha e^{-i\theta})$  and  $\tilde{p}_\theta = i2^{-1/2}(\alpha^* e^{i\theta} - \alpha e^{-i\theta})$ . The pattern function shows the typical features of the quadrature distribution.

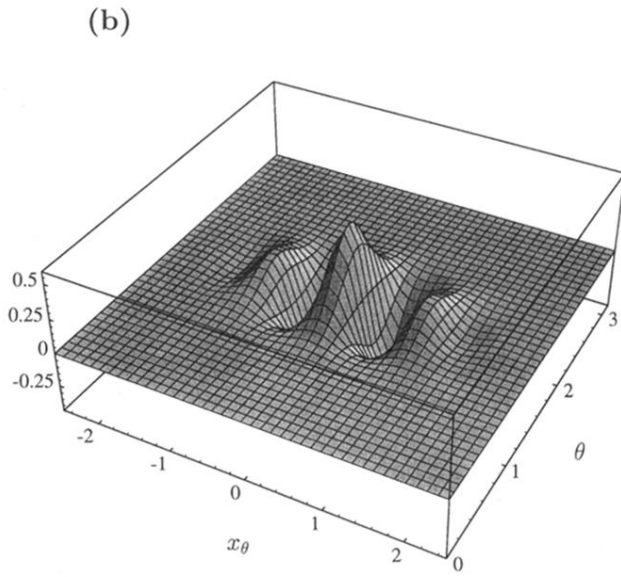
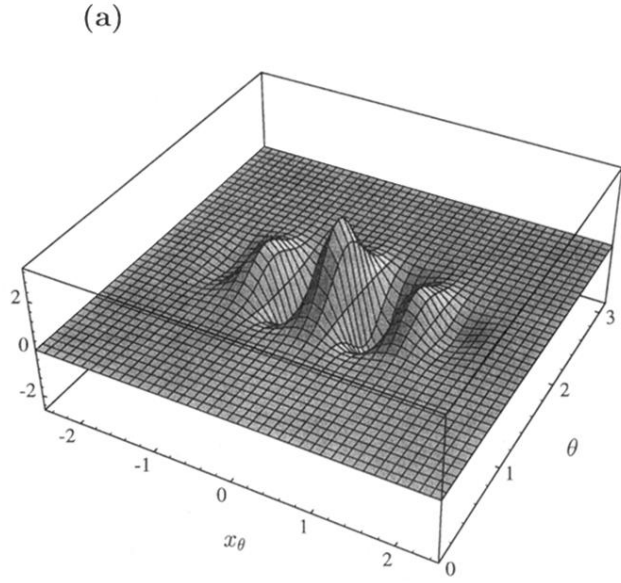


FIG. 2. Real part of the off-diagonal pattern function  $F_{\alpha, -\alpha}(x_\theta, \theta)$  (a) versus the real part of the wave-function product  $\psi_\alpha^*(x_\theta, \theta)\psi_{-\alpha}(x_\theta, \theta)$  (b) for  $\alpha=4$ . The figures are almost indistinguishable.